Chapter 2: Analysis of Key Protein Properties for the Comparison of Transmembrane Proteins (MembComp)

1.0 ABSTRACT

With new methods being developed to create theoretical structures of transmembrane proteins, key features need to be analyzed to determine the similarity and health of these competing structures. Transmembrane proteins share a distinct geometric shape similar to that of a barrel with the wall created through secondary structures. The alignment and position of these secondary structures allows for a central system for measuring common characteristics to be setup.

Using the planar alignment of the alpha-helices found in GPCRs, key characteristics are determined and analyzed for Rhodopsin and Bacteriorhodopsin crystal structures. The key characteristics found are: Helical bend, Helical tilt, HPM angle, Phobic face, and three characteristics to describe helical position. These characteristics are then measured and compared for the crystal structures of Rhodopsin and Bacteriorhodopsin.

2.0 INTRODUCTION

Transmembrane proteins play an important role in the communication of the cell to the outside world. A major class of transmembrane proteins is the G-protein coupled receptors (GPCRs) that are receptors for neurotransmitters, neuropeptides, and are present in sensory neurons. An understanding of the similarities and differences between these proteins would lend to a better understanding of the functions of each transmembrane protein.

These proteins show a high level of symmetry and organization in the portion of their structures that reside within the transmembrane (TM) domain. Bacteriorhodopsin

having seven alpha helices in a barrel and Porin having many beta sheets that form an enclosed structure (beta barrel) are examples of the kind of structural organization of transmembrane proteins. This paper will focus on the comparison of alpha helical TM proteins, but the methods and characteristics found in this paper can also be applied to beta barrels.

Visualization of these proteins shows that there are common structural elements and similarities that can not be seen in a simple RMS comparison of the positions of the C-alpha atoms (CRMS) or of the main chain atoms (MRMS). This measurement of the differences of two proteins is only specific enough to answer the question of weather two protein are different, but not give any indication of how or where. This creates a need for specific characteristics to be developed that describe the general character of the TM protein structures.

In order to compare two structures, a common coordinate system needs to exist between the two structures that allows for comparison of the same structural elements. Since these proteins reside in a lipid membrane, the main secondary structures of the protein maintain the best possible interactions with the lipid membrane. The best interactions for the core hydrophobic middle of each secondary structure are in the same plane as the lipid bilayer. This results in all the core secondary structures found in the transmembrane regions of the protein residing in the same plane together (1).

This plane gives a specific comparable location for all transmembrane proteins, since the barrel of these proteins can produce infinite planes along its length. This allows us to define comparable characteristics from this plane (referred to as the plane of intersection in this paper). The characteristics derived from this plane of intersection

are: Helical bend, Helical tilt, HPM angle, Phobic face, and other characteristics to describe helical position. These characteristics were then measured and compared for Rhodopsin and Bacteriorhodopsin crystal structures.

3.0 METHODS

The parameters that would be most informative for the researcher are those that describe the properties of the main structural elements of the membrane protein. The two main structural elements are beta sheets and alpha helices that are positioned perpendicular to the cell membrane. Utilizing this knowledge, a cross section of the protein is sliced parallel to the cell membrane to create a plane that intersects all main TM structural elements of the protein (see Figure 1). This plane can be set anywhere along the vertical axis (the axis that runs along the protein from the intracellular region to the extracellular region) of the protein, but in order to have a consistent and comparable plane in all proteins it is placed it along the hydrophobic centers of the helices. This placement of the plane of intersection gives a nice coordinate system for the reference of specific GPCR parameters in a two dimensional environment.

These parameters describe the overall shape and placement of the core secondary structures found in the transmembrane regions (alpha helices for GPCRs). These parameters are: Helical bend, Helical tilt, HPM angle, Phobic face, and other characteristics to describe helical position.

3.1 Definition of the Hydrophobic Centers

In order to have a consistent common location used on each helix to find the plane of intersection, the point of maximum hydrophobicity needs to be calculated. This is done using a similar approach as the TM2ndS (2-3) method developed in the Goddard lab

at Caltech. These centers have been found and validated for the rhodopsin crystal structure (2), and for the predicted structures of human β1 and β2 adrenergic receptors (4), the human dopamine D2 receptor (5), and several olfactory recptors (6-8).

Using the fact that the middle of the protein is helical and immersed in a lipid bilayer (membrane), these regions will have a larger grouping of hydrophobic residues with the center being near the middle of the membrane (1). TM2ndS looks for these conserved hydrophobic portions of the protein sequence to be assigned the helical TM regions. This is accomplished through the following steps:

1) A multiple sequence alignment is created using a NCBI Blast search (9-10) on the SwissProt database and filtering out those hits less than a 200 bit score. ClustalW (11) would then align the sequences and an even distribution of sequences from 100 to 20 percent homology would be kept for the final alignment.

2) The SeqHyd hydrophobic profile algorithm would then be used to create an averaged hydrophobic score across the entire alignment. This score would be averaged over a range of nearest neighbors in the sequence alignment, and the size of this range will be called the window size (i.e., a range of 5 on each side of the target residue will be window size 10). The profiles generated from window sizes 12 to 30 would be analyzed for seven distinct hydrophobic peaks using a baseline derived from the global average of the profile (+/- 0.05 of the baseline choosing the closest to the average). The lowest window size that yields seven peaks is used to determine the ends of the TM regions by finding where the peaks cross the baseline.

3) A fine grain prediction of the TM regions is then done using the TM2ndS helix capping program. This will look for helix breaking residues or charged residues and alter

the ends of the TM region up to 4 residues on each side (minumin 21 residues) to exclude these.

4) The target's alignment hydrophobic profile from Step 2) is now used to find the highest point of hydrophobicity in each TM region. The profile is averaged over varying lengths (12 to 30 residues) and each hydrophobic peak is analyzed and the largest group of nearest peaks is averaged to give the hydrophobic center.

3.2 Development of the Plane of Intersection

The plane of intersection will be aligned to the hydrophobic centers of the helices located in the TM region of the GPCR. While the alignment of a plane to three non-collinear points is rudimentary, there is a little bit more involved in aligning a plane to seven points (for GPCRs, but this approach can be used on any number of points 3 or greater). To do this we will utilize a Least Squares Approach in a three dimensional system.

First we will define the problem as wanting to minimize the maximum error value of the planar approximation defined by the equation: $Ax_i + By_i + D = z_i$ where (x_i, y_i, z_i) is the coordinates of the center point *i.* We will let *m* equal the number of points to minimize the distance.

$$\min \max_{i=1,2,3,..,m} \{|z_i - (Ax_i + By_i + D)|\} \qquad (1)$$

To approach this problem we set it up as a least squares minimization problem of A, B, and C.

$$\sum_{i=1}^{m} [z_i - (Ax_i + By_i + D)]^2 \qquad (2)$$

Now to set up the minimization equations:

$$
\begin{aligned}
0 &= \frac{\partial}{\partial A}\sum_{i=1}^{m}\left[z_i-\left(Ax_i+By_i+D\right)\right]^2 = 2\sum_{i=1}^{m}\left(z_i-Ax_i-By_i-D\right)\left(-x_i\right)\\
0 &= \frac{\partial}{\partial B}\sum_{i=1}^{m}\left[z_i-\left(Ax_i+By_i+D\right)\right]^2 = 2\sum_{i=1}^{m}\left(z_i-Ax_i-By_i-D\right)\left(-y_i\right) \qquad (3)\\
0 &= \frac{\partial}{\partial D}\sum_{i=1}^{m}\left[z_i-\left(Ax_i+By_i+D\right)\right]^2 = 2\sum_{i=1}^{m}\left(z_i-Ax_i-By_i-D\right)\left(-1\right)
\end{aligned}
$$

Now rearrange the equations (3) into a system of solvable equations:

$$
\begin{aligned}
\sum_{i=1}^{m} z_i x_i &= A\sum_{i=1}^{m} x_i^{\,2} + B\sum_{i=1}^{m} y_i x_i + D\sum_{i=1}^{m} x_i\\
\sum_{i=1}^{m} z_i y_i &= A\sum_{i=1}^{m} x_i y_i + B\sum_{i=1}^{m} y_i^{\,2} + D\sum_{i=1}^{m} y_i \qquad (4)\\
\sum_{i=1}^{m} z_i &= A\sum_{i=1}^{m} x_i + B\sum_{i=1}^{m} y_i + Dm
\end{aligned}
$$

which results in the following solutions:

$$
\begin{aligned}
A &= -\frac{\left(\begin{array}{l}
-\sum_{i=1}^{m} y_i z_i \sum_{i=1}^{m} x_i \sum_{i=1}^{m} y_i - \sum_{i=1}^{m} x_i \sum_{i=1}^{m} z_i \sum_{i=1}^{m} y_i^{\,2} - m\sum_{i=1}^{m} x_i y_i \sum_{i=1}^{m} y_i z_i\\
-\left(\sum_{i=1}^{m} y_i\right)^2 \sum_{i=1}^{m} x_i z_i + m\sum_{i=1}^{m} x_i z_i \sum_{i=1}^{m} y_i^{\,2} + \sum_{i=1}^{m} z_i \sum_{i=1}^{m} y_i \sum_{i=1}^{m} x_i y_i
\end{array}\right)}{\left(\begin{array}{c}
-m\sum_{i=1}^{m} x_i^{\,2}\sum_{i=1}^{m} y_i^{\,2} + m\left(\sum_{i=1}^{m} x_i y_i\right)^2 + \left(\sum_{i=1}^{m} x_i\right)^2 \sum_{i=1}^{m} y_i^{\,2}\\
-\sum_{i=1}^{m} x_i y_i \sum_{i=1}^{m} x_i \sum_{i=1}^{m} y_i + \sum_{i=1}^{m} x_i^{\,2}\left(\sum_{i=1}^{m} y_i\right)^2 - \sum_{i=1}^{m} x_i \sum_{i=1}^{m} y_i \sum_{i=1}^{m} x_i y_i
\end{array}\right)}\\
B &= \frac{\left(\begin{array}{l}
-\sum_{i=1}^{m} x_i y_i \sum_{i=1}^{m} x_i \sum_{i=1}^{m} z_i + m\sum_{i=1}^{m} x_i y_i \sum_{i=1}^{m} x_i z_i - m\sum_{i=1}^{m} x_i^{\,2}\sum_{i=1}^{m} y_i z_i\\
+\left(\sum_{i=1}^{m} x_i\right)^2 \sum_{i=1}^{m} y_i z_i + \sum_{i=1}^{m} y_i \sum_{i=1}^{m} x_i^{\,2}\sum_{i=1}^{m} z_i - \sum_{i=1}^{m} x_i \sum_{i=1}^{m} y_i \sum_{i=1}^{m} x_i z_i
\end{array}\right)}{\left(\begin{array}{c}
-m\sum_{i=1}^{m} x_i^{\,2}\sum_{i=1}^{m} y_i^{\,2} + m\left(\sum_{i=1}^{m} x_i y_i\right)^2 + \left(\sum_{i=1}^{m} x_i\right)^2 \sum_{i=1}^{m} y_i^{\,2}\\
-\sum_{i=1}^{m} x_i y_i \sum_{i=1}^{m} x_i \sum_{i=1}^{m} y_i + \sum_{i=1}^{m} x_i^{\,2}\left(\sum_{i=1}^{m} y_i\right)^2 - \sum_{i=1}^{m} x_i \sum_{i=1}^{m} y_i \sum_{i=1}^{m} x_i y_i
\end{array}\right)} \qquad (5)
\end{aligned}
$$

$$D = -\frac{\left(\begin{array}{c}\sum_{i=1}^{m} y_i z_i \sum_{i=1}^{m} x_i \sum_{i=1}^{m} x_i y_i - \sum_{i=1}^{m} x_i \sum_{i=1}^{m} x_i z_i \sum_{i=1}^{m} y_i^{\,2} + \sum_{i=1}^{m} y_i \sum_{i=1}^{m} x_i y_i \sum_{i=1}^{m} x_i z_i \\ - \sum_{i=1}^{m} y_i \sum_{i=1}^{m} x_i^{\,2} \sum_{i=1}^{m} y_i z_i + \sum_{i=1}^{m} x_i^{\,2} \sum_{i=1}^{m} z_i \sum_{i=1}^{m} y_i^{\,2} - \sum_{i=1}^{m} z_i \left(\sum_{i=1}^{m} x_i y_i\right)^2\end{array}\right)}{\left(\begin{array}{c}-m \sum_{i=1}^{m} x_i^{\,2} \sum_{i=1}^{m} y_i^{\,2} + m\left(\sum_{i=1}^{m} x_i y_i\right)^2 + \left(\sum_{i=1}^{m} x_i\right)^2 \sum_{i=1}^{m} y_i^{\,2} \\ - \sum_{i=1}^{m} x_i y_i \sum_{i=1}^{m} x_i \sum_{i=1}^{m} y_i + \sum_{i=1}^{m} x_i^{\,2} \left(\sum_{i=1}^{m} y_i\right)^2 - \sum_{i=1}^{m} x_i \sum_{i=1}^{m} y_i \sum_{i=1}^{m} x_i y_i\end{array}\right)}$$

The solution above gives the plane of intersection where we let C=1 and get it to $Ax_i + By_i + Cz_i + D = 0$.

3.3 Definition of a coordinate system on the Plane of Intersection

With the plane of intersection found and aligned to the seven hydrophobic centers of the protein, an origin and axis must be setup that will be comparable for all proteins. The origin of the plane of intersection is the center of the protein, which is the geometric center of the centers defined for each of the helices, is then projected onto the plane of intersection. With the origin defined, the Y-axis is defined as the line created from the origin to the defined center of helix 1 (geometric or hydrophobic) that has been projected onto the smallest moment of inertia (generally the middle of the helical barrel) and then projected onto the plane.

The positive Y-axis is the defined as the segment of the Y-axis from the origin to and past the center of helix 1. The X-axis is defined as the line perpendicular to the Y-axis that intersects the Y-axis at the origin. The positive X-axis is defined as the side of the axis from the origin that is nearest to the center of helix 7 (for GPCRs, or sequentially the last secondary structure in the TM region). Lastly, the positive Z-axis is defined as

the segment of the axis from the origin that heads towards the extracellular region of the protein.

This system defines a two-dimensional view of the protein from the extracellular region looking down towards the protein. Helix 1 is located at the top of this view with the helices located counter-clockwise in a circular direction.

3.4 Definition of the Key Properties

Each of the key properties is measured on the plane of intersection as described above and on a common plane specific to each helix. This common plane is defined by locating the origin at the center of the helix that has been projected onto the smallest moment of inertia. The Z-axis is along the smallest moment of inertia and the x-axis is formed by the line connecting the center of the protein projected onto the plane to the center of the helix. This common helical plane gives us another look at helix specific information in a common frame of reference as any other membrane protein (13-14 use the common plane of helix 5 for building rhodopsin). Since both the plane of intersection and the common helical plane can be used for determination of the key properties, the plane chosen will be referred to as the plane of analysis.

3.4.1 Helical Bend

The bend of the helix is determined by the angle defined by the following three points:

1. The geometric center of the top (extracellular) four residues in the helix.
2. The geometric center of the four residues closest to the plane of analysis and projected onto the plane.
3. The geometric center of the bottom (intracellular) four residues in the helix.

The helical bend is equal to 180 – {angle of three above points} degrees. In this fashion the greater the bend or distortion from a straight line, the larger the helical bend. This gives an overall idea of how far the top and bottom of the helix are from the center of the helix with respect to the plane of analysis.

3.4.2 Helical Tilt

The tilt of the helix is a measurement how far a helical barrel is from being perpendicular to the plane of analysis. This will give a sense of how vertical and horizontal a helix is in relationship to the rest of the protein. The tilt is determined by measuring the angle of these three points:

1. The geometric center of the top (extracellular) four residues in the helix.
2. The geometric center of the 4 residues closest to the plane of analysis and projected onto the plane.
3. The projected geometric center of the helical centers.

The helical tilt is equal to 90 – {angle of above three points} degrees. The geometric top point is used, since the bottom tilt is equal to the tilt +/- the helical bend.

3.4.3 HPM Angle

The hydrophobic angle is a measurement of the rotation of the helix with respect to the protein. This rotation is with respect to the overall hydrophobic character of the helix, and not the exact rotation of the C-alpha atoms. The hydrophobic angle gives a measurement of how far the hydrophobic moment of the helix is from pointing directly away from the center of the protein. This is important since the hydrophobic moment tends to point towards the lipid (a HPM angle of zero). The hydrophobic angle is determined using the following points:

1. The point found at the end of the hydrophobic vector and projected onto the plane of intersection. This point is obtained one of two ways:
    a) The vector addition of all vectors created from the line made from the C-alpha atom to the geometric center of the non-hydrogen sidechain end atoms (traditional way to calculate hydrophobic moments) for each residue (centered around the helical center). The length of each of the vectors is determined by a predetermined hydrophobic scale. The eisenberg scale is used in this paper (12).
    b) The projection of each residue's C-alpha atom of the helix on the common helical plane and assigning each point the value determined by the hydrophobic scale. Each point is then projected onto a circle of radius 1, then finding the arc angle equal to the Face angle (see key properties below) corresponding to this angle that contains the largest sum of all residues found inside. The middle of this arc is assigned to the angle of the vector and the sum of the scale values of each point is assigned to the length of this vector. This is used to determine the direction of the most hydrophobic canonical side of the helix. This method is not used in this paper since it works best with perfectly canonical helices, but it is the first rotational optimization step of MembStruk (2, 8).
2. The helical center point projected onto the plane and the smallest moment of inertia.
3. The geometric center of all helical centers projected onto the plane of analysis.

The HPM angle is equal to 180 – {angle of the above three points} with positive angles defined as angles that are rotated counter clockwise from the extracellular viewpoint.

3.4.4 Phobic Face angle

The phobic face angle is a measurement of how much of the helical barrel faces the lipid bilayer. The measurement is an angle that represents the size of the arc around the helix which can interact with the lipid. This measurement is obtained by projecting onto the common helical plane the positions of the C-alpha atoms and then connecting the atoms of each of the TM regions together. Then each of the atoms positions are converted into cylindrical coordinates and their radii are set equal to 1 angstom. The circle about the origin is searched to locate a gap between the helical lines, and the angle of the largest gap is defined as the phobic face angle (see Figure 2).

3.4.5 Characteristics to measure placement of Helical Centers

The centers of the helices are defined by three descriptors: 1) An angle of rotation away from the Y-axis (with helix one always at zero). 2) A distance the center of the helix is from the geometric center of all helices. 3) The distance the center is from the plane of analysis. The first two descriptors are cylindrical coordinates that define the placement of the helices on the graph of the plane of analysis, and the third is an indication of how well each helix aligned to the plane.

3.4.6 Other measured properties

There are three other properties that are measured by MembComp. The first is the projected magnitude of the HPM vector, so that the overall strength of the hydrophobic character of the helix on the plane of analysis is known. The second is the projected fit of the HPM vector to the plane of intersection, giving an idea of the Z-

direction the vector was pointing (positive going towards extracellular). The last property measured is the bisector angle. The bisector angle is the degree of rotation needed to place the HPM vector from the zero position to the center of the Phobic Face angle. The bisector angle is calculated as comparison to other membrane building programs that use this angle to define the rotation of the helices (13-14).

4.0 RESULTS

Using the described methods above, key properties were found for the crystal structures of bovine rhodopsin and bacteriorhodopsin. In all cases the hydrophobic scale used was the Eisenberg scale, and the HPM vector was calculated using Method 3.4.3 1) a) vector addition.

4.1 Hydrophobic centers for Rhodopsin and Bacteriorhodopsin

Two sets of hydrophobic centers were defined for the bovine rhodopsin protein. The first set of hydrophobic centers were defined using the method in Section 3.1 and have been already published (1). The second set of centers was created from the initial information created from the first set of hydrophobic centers. This second set of centers was made to correspond more closely to the same method used to get a good set of centers for bacteriorhodopsin.

This second set was obtained by taking the average window outputs that were averaged in the previous paper and instead giving the sum for each residue over the window sizes of 16 to 24. Since the larger the window size the smaller the overall peaks, this gave a larger weight to the lower window sizes. This averaged window graph was then analyzed for the two largest peaks by calculating the change in slope of the graph (see Figure 3). These centers aligned to a plane with an RMS of 0.5354 on the 1HZX

structure. This same method was used for defining the hydrophobic centers of bacteriorhodopsin.

For bacteriorhodopsin the following sequences were aligned to produce the hydrophobic graphs:

```
1BRX
P1;gi|15790468|ref|NP_280292.1|
P1;gi|3023375|sp|P96787|BAC3_HALS
P1;gi|114807|sp|P19585|BAC1_HALS1
P1;gi|231626|sp|P29563|BAC2_HALS2
P1;gi|2829812|sp|P94854|BACR_HALV
P1;gi|2499386|sp|Q57101|BACR_HALA
P1;gi|2499387|sp|Q53496|BACR_HALS
P1;gi|14194473|sp|O93740|BACR_HAL
```

These nine sequences were found through a blast search (9-10) of the swissprot database, and then aligned using ClustalW (11). This alignment was run through the TM2NDS program (1) and the final window sizes were summed for a TM prediction (see Figure 4). Each helix was individually analysed for the best range of window sizes. The two largest peaks were then analyzed to determine which peak is best for alignment to a plane (Figure 5). The TM regions used were obtained from the crystal structure 2BRD and the final HPM centers were: 20.3806, 50.7112, 89.8305, 114.8941 (second largest peak), 146.067, 181.7722, and 213.7167. These centers align to a plane with an RMS of 0.4354 to the 1CRW crystal structure. These centers were tested on other bacteriorhodopsin structures with the following results:

```
PDB    RMS fit to Plane
----   ----------------
1BRX - 0.4200 (28-MAY-98)(2.3 A, RET)
1AT9 - 0.4270 (20-AUG-97)(3.0 A, RET)
1C3W - 0.4354 (28-JUL-99)(1.55 A, lipid, RET)
2BRD - 0.4656 (27-DEC-95)(3.5 A, RET, DPG)
1AP9 - 0.4686 (26-JUL-97)(2.5 A, RET)
1BM1 - 0.5167 (28-JUL-98)(3.5 A, DPG, RET)
```

```
1FBK - 0.5878 (15-JUL-00)(3.2 A, RET)
1I15 - 0.7205 (30-JAN-01)(Theoretical model,
                          D2 modeled on Bacteriorhodopsin)
1L0M - 1.2210 (11-FEB-02)(SOLUTION NMR DATA used)
```

Surprisingly, even a D2 theoretical model that was built from Bacteriorhodopsin had these aligned centers fit well to a plane. This shows the dependence of a homology model to the original structure.

4.2 Rhodopsin Key Properties

The key properties for 1HZX bovine rhodopsin are (using the second set of hydrophobic centers):

Plane of Intersection Table

		Helical Bend	Plane Tilt	Proj. HPM Angle	Proj. HPM Magn.	Proj. HPM Fit	Plane CM Dist.	Plane CM Angle	Proj. CM Fit
HELIX	1	17.9	36.9	-29.0	3.3	0.3	14.9	0.0	0.4172
HELIX	2	3.6	22.0	33.0	2.9	-5.6	9.0	41.1	0.2588
HELIX	3	13.8	21.0	-78.5	3.1	2.0	3.8	139.0	0.4706
HELIX	4	12.6	5.7	-57.7	1.8	-1.3	11.8	126.5	-0.6978
HELIX	5	25.8	17.2	78.6	1.1	4.7	14.4	189.3	0.4363
HELIX	6	31.4	30.2	-103.0	1.4	-3.2	10.2	251.6	-0.0450
HELIX	7	36.8	38.7	-11.6	3.8	1.9	8.1	313.8	-0.9301
RMS		23.0	26.8	63.7	2.7	3.2	10.9		

Centered Plane Table

		HPM Angle	HPM Magn.	Helical Bend	P. Face Deg.	Bisector Angle	
HELIX	1	-19.9	4.0	16.7	228	-2.54	(2- 7)
HELIX	2	3.5	5.6	5.0	141	22.14	(1- 4)
HELIX	3	-47.7	3.8	11.1	34	18.89	(4- 5)
HELIX	4	-49.8	3.8	23.8	220	-36.43	(2- 3)
HELIX	5	86.6	6.0	6.4	229	5.99	(3- 6)
HELIX	6	-85.6	4.6	29.1	173	-0.03	(5- 7)
HELIX	7	-6.8	3.9	33.6	140	-8.00	(6- 1)
RMS		53.5	4.6	20.7		18.05	

These results show some interesting characteristics about bovine rhodopsin. The helices 3, 5 and 6 show some deviation in the positioning of the HPM vectors from pointing towards the lipids. This is easily seen in the graph of these properties in Figure

6. Helix 3 is pointing between helices 4 and 2 which is right in the largest phobic face gap, and actually uses both sides of its helix to interact with the lipid.

Helix 3 tilts in such a way that the top half of the helix is closer to the helices 2, 4 gap and the bottom half of helix 3 is closer to the helices 4, 5 gap (Figure 7). The extracellular top half of helix three has a 90 degree shift in its hydrophobic character from the intracellular bottom half. In this fashion, helix 3 can interact with the lipid in two different locations due to its tilt. This property is key in defining the rotation of helix 3 in rhodopsin.

Helix 6 has its hydrophobic character pointing in the direction of helix 5, and helix 5 is pointing towards helix 6. This rotation for helix 6 is explained in part by the closing of the EC2 loop in the binding of cis-retinal (1). There is also evidence that this is one of two possible low energy conformations for helix 6 (15).

The rotations of helix 3 and 6 are important to the binding of cis-retinal, since slight changes in the rotation of either can dramatically alter the shape of the binding site. This can be seen in figure 8, which shows the key residues involved in the binding site as graphed on the plane of intersection. Rhodopsin might in fact rotate both helix 3 and 6 in order to create the binding site seen in Figure 8, while one theoretical structure shows rhodopsin with helix 3 and 6 rotated -90 degrees (15). This open (no cis-retinal bound) structure has the salt bridge Glu 122 (TM 3) – Lys 296 (TM 7) which completely closes off this binding site. The rotations of helix 3 and 6 are believed to be tied to the closing of the EC2 loop during the binding of cis-retinal.

The bisector angle (shown as the number of degrees away from the zero angle on the common helical plane) computed for bovine rhodopsin shows that for helices 1, 5, 6,

and 7 there was not much deviation from the optimal location defined as zero for each helix. However, on helices 2, 3, and 4 there is a significant difference. The equation (HPM vector) – (bisector angle) gives the amount of rotation needed to place the HPM vector at the bisection of the angle between the two nearest helices (the parenthesis contain the helices used to calculate this angle). Using this equation, helix 2 improves in its rotation but helices 3 and 4 get worse suggesting that the current method in MembStruk of using the zero angle does produce better initial rotations than those suggested in other methods (14).

4.3 Rhodopsin Simulation Analysis

Simulations were run on the 1F88 bovine rhodopsin crystal structure to test the stability of the helical regions and the loop regions (16). These simulations were carried out with an explicit bilipid layer and explicit waters. The rhodopsin crystal structure was placed in a simulation box containing 256 Dipalmitoyl Phosphatidyl Choline (DPPC) molecules and bulk water. Four structures were created for the simulation: 1) The crystal structure with cis-retinal (Crystal), 2) The crystal structure without cis-retinal (Cry-wo), 3) A trunctated crystal structure missing the N and C-terminus and without cis-retinal (Cry-trun), and lastly 4) The crystal structure TM regions without loops, without cis-retinal, and without the N and C-terminus. The simulations were carried out using the GROMACS code (17) for up to 584 picoseconds of dynamics simulation (Cry-TM).

MembComp was used to analyze the changes in the helices during the simulation. The helical bend, helical tilt, and HPM vector were all calculated for specific snapshots (0, 200, 248, 296, 344, 392, 440, 488, 536, and 584 ps) that were taken during the simulation. The TM region used was the TM region from the crystal structure 1F88, and

the published (1) first set of hydrophobic centers were used in the calculation of the key properties. The HPM vector was calculated on the common helical plane. These properties are plotted against time in Figures 9-11.

The full crystal structure with cis-retinal was overall able to maintain the original TM position and shape better than the other structures. This structure also appeared to be converging to a common shape in helical bends and tilts. Only helix 4 had a significant overall gain of +20 to its HPM angle while all the other helices stabilized the change in their angles. Helices 1, 2, 4, 5, and 7 all began to stabilize their helical bends around 26 degrees suggesting that this might be an optimal conformational shape for the helices, while 3 got straighter and 6 got more bent. The helices 1, 3, 5, 6, and 7 began to cluster again around 30 degrees for helical tilt while helices 2 and 4 remains near their starting positions.

The full crystal structure without cis-retinal (Cry-wo), while it had not altered its overall shape, did not appear to be converging to any specific shape. Only helix 1 had a significant overall change in its HPM angle with helix 1 gaining +50 degrees. Helices 1 and 4 were the only helices to change their helical bends both becoming more bent. There was significant change in the tilts, as helices 4, 5, 6, and 7 all increased their tilts by 10 degrees or more. This suggests that the ligand cis-retinal has a stabilizing effect on the rhodopsin structure. Looking at the changes in both Crystal and Cry-wo, helix 4 seems to have the ability to alter its conformation the most with or without ligand.

The two partial structures (Cry-trun, Cry-TM) both show the destabilizing effect missing the loops and termini can be. Helix 2 changed the most in its helical bend and

tilt for Cry-trun, while all the helices on Cry-TM has significant changes in their bends and tilts.

4.4 Bacteriorhodopsin

The summed hydrophobic centers were used to obtain the following calculated properties for bacteriorhodopsin (1C3W):

Plane of intersection Table

	Helical Bend	Plane Tilt	Proj. HPM Angle	Proj. HPM Magn.	Proj. HPM Fit	Plane CM Dist.	Plane CM Angle	Proj. CM Fit
HELIX 1	6.3	24.1	-95.9	5.1	4.4	14.7	0.0	-0.5727
HELIX 2	6.9	16.8	101.1	3.3	-2.3	10.0	34.4	-0.8442
HELIX 3	15.9	15.5	5.4	2.3	3.2	5.0	100.6	0.0813
HELIX 4	4.0	19.5	-101.5	1.4	-3.3	12.1	150.3	-0.4151
HELIX 5	10.8	1.8	-156.1	1.6	4.8	13.7	191.2	0.0879
HELIX 6	8.5	5.1	123.1	5.2	-0.4	9.2	243.9	-0.2809
HELIX 7	19.9	25.1	-39.4	2.6	0.9	8.2	316.2	0.1440
RMS	11.6	17.5	100.6	3.4	3.2	10.9		

Centered Plane Table

	HPM Angle	HPM Magn.	Helical Bend	P. Face Deg.	Bisector Angle	
HELIX 1	-91.5	5.9	0.0	229	-4.73	(2- 7)
HELIX 2	99.2	4.3	2.9	172	15.94	(1- 3)
HELIX 3	23.4	4.8	5.5	116	-8.30	(2- 4)
HELIX 4	-149.0	5.2	3.5	190	-4.37	(3- 5)
HELIX 5	-174.5	5.1	4.3	216	5.92	(4- 6)
HELIX 6	123.9	5.5	3.9	181	9.77	(5- 7)
HELIX 7	-32.4	3.4	25.1	161	-14.22	(6- 1)
RMS	112.0	4.9	10.1		9.98	

These properties show that bacteriorhodopsin has a unique placement of its hydrophobic character, with helices 2, 3, and 4 pointing toward the same location and helices 1 and 7 also pointing towards a common location. Helix 5 appears to be pointing towards the center of the protein and helix 6 is pointing directly at helix 7 (Figure 12).

The differences between the bacteriorhodopsin various crystal structures and 1C3W were computed and the averages are shown below (plotted in Figure 12):

Negative numbers represent the structure smaller than 1C3W
Negative degrees is counter-clockwise from the 1C3W

Plane of Intersection Average Difference Table

	Helical Bend	Plane Tilt	Proj. HPM Angle	Proj. HPM Magn.	Proj. HPM Fit	Plane CM Dist.	Plane CM Angle	Proj. CM Fit
1BRX	2.8	1.8	21.1	1.2	0.8	0.2	0.6	0.0385
1AT9	2.7	2.2	16.9	1.1	0.9	0.2	0.9	0.0770
2BRD	1.8	2.3	26.9	1.0	1.1	0.2	0.9	0.0693
1AP9	2.8	2.0	22.1	1.0	0.9	0.3	0.9	0.1052
1BM1	1.6	1.8	14.9	0.9	0.8	0.2	1.1	0.0814
1FBK	3.8	2.6	13.0	1.0	0.7	0.3	0.9	0.4390
1I15	4.8	4.8	89.8	2.6	1.5	0.2	2.4	0.3069
1L0M	12.4	7.7	49.0	1.6	1.8	0.9	3.1	1.3030

Comparision Plane Average Difference Table

	HPM Angle	HPM Magn.	Helical Bend	P. Face Deg.
1BRX	27.9	1.1	5.2	4
1AT9	22.8	1.2	4.2	4
2BRD	27.5	1.3	2.0	5
1AP9	20.5	1.2	4.4	4
1BM1	15.0	1.2	2.3	4
1FBK	20.7	1.3	3.6	6
1I15	104.0	1.7	5.0	8
1L0M	50.9	1.7	13.9	17

The last two structures are interesting to note, having HPM angles in the more common location of pointing directly away from the center of the protein for helices 4, 5, and 6 (Figure 13). This difference in placement of the hydrophobicity for the 1L0M structure might be due to the binding of retinal in the other structures, since the binding site is next to helices 3, 4, 5, and 6 (Figure 14).

Of particular interest are the differences between 1C3W and 1I15 (D2 theoretical structure), so the complete set of differences is shown below:

Negative numbers represent the structure smaller than 1C3W
Negative degrees is counter-clockwise from the 1C3W

Plane of Intersection Difference Table

	Helical Bend	Plane Tilt	Proj. HPM Angle	Proj. HPM Magn.	Proj. HPM Fit	Plane CM Dist.	Plane CM Angle	Proj. CM Fit

HELIX	1	-3.3	3.5	-9.2	-2.5	0.8	0.2	0.0	0.0568
HELIX	2	1.6	-8.5	103.4	-3.1	-0.4	0.1	0.6	-0.1405
HELIX	3	-11.7	-5.8	19.0	-3.6	-0.8	0.1	9.1	-0.0383
HELIX	4	-1.4	-5.3	141.6	1.1	1.7	0.3	-3.1	-0.7938
HELIX	5	-3.9	5.2	178.8	3.0	-5.9	0.1	-0.1	1.0289
HELIX	6	11.5	3.0	-139.6	-4.8	0.5	0.4	3.6	-0.0576
HELIX	7	0.5	2.1	36.9	-0.4	0.6	0.1	-0.5	0.0322
AVERAGE		4.8	4.8	89.8	2.6	1.5	0.2	2.4	0.3069

Comparision Plane Difference Table

		HPM Angle	HPM Magn.	Helical Bend	P. Face Deg.	Bisector Angle	
HELIX	1	-47.6	-1.1	4.8	11	0.09	(2-7)
HELIX	2	167.3	-1.5	11.5	8	3.94	(1-3)
HELIX	3	6.0	-2.7	2.1	-4	-10.32	(2-4)
HELIX	4	-160.2	-0.2	1.2	25	7.55	(3-5)
HELIX	5	-166.9	-2.7	-6.1	-2	0.37	(4-6)
HELIX	6	-126.2	-3.6	6.1	8	-3.84	(5-7)
HELIX	7	54.0	0.0	-2.9	2	2.21	(6-1)
AVERAGE		104.0	1.7	5.0	8		

The main differences in the two structures come in the direction of the HPM angles on helices 2, 4, 5, and 6. This is especially interesting since the rest of the structure conforms well to the 1C3W structure. The direction that these helices are pointing is more in the direction of rhodopsin, which would be necessary since D2's binding site is located near TM regions 3, 4, 5, and 6 (5). This suggests that while this structure might have the binding site correctly modeled, the rest of the structure still remains similar to bacteriorhodopsin.

4.5 Comparision of Bovine Rhodopsin to Bacteriorhodopsin

Now having computed the key properties for rhodopsin and bacteriorhodopsin, the differences between the two can be analyzed. Below are the difference tables of 1HZX and 1C3W:

Negative numbers represent the structure smaller than 1C3W
Negative degrees is counter-clockwise from the 1C3W

Plane of Intersection Difference Table

	Helical Bend	Plane Tilt	Proj. HPM Angle	Proj. HPM Magn.	Proj. HPM Fit	Plane CM Dist.	Plane CM Angle	Proj. CM Fit
HELIX 1	11.6	12.8	66.9	-1.8	-4.1	0.2	0.0	0.9899
HELIX 2	-3.3	5.2	-68.1	-0.4	-3.3	-1.0	6.7	1.1030
HELIX 3	-2.1	5.5	-83.9	0.8	-1.2	-1.2	38.4	0.3893
HELIX 4	8.6	-13.8	43.8	0.4	2.0	-0.3	-23.8	-0.2827
HELIX 5	15.0	15.4	-125.3	-0.5	-0.1	0.7	-1.9	0.3484
HELIX 6	22.9	25.1	133.9	-3.8	-2.8	1.0	7.7	0.2359
HELIX 7	16.9	13.6	27.8	1.2	1.0	-0.1	-2.4	-1.0741
AVERAGE	11.5	13.1	78.5	1.3	2.1	0.6	11.6	0.6319

Comparision Plane Difference Table

	HPM Angle	HPM Magn.	Helical Bend	P. Face Deg.	Bisector Angle
HELIX 1	71.6	-1.9	16.7	-1	2.19 (2-7)
HELIX 2	-95.7	1.3	2.1	-31	Diff. Bisect.
HELIX 3	-71.1	-1.0	5.6	-82	Diff. Bisect.
HELIX 4	99.2	-1.4	20.3	30	Diff. Bisect.
HELIX 5	-98.9	0.9	2.1	13	Diff. Bisect.
HELIX 6	150.5	-0.9	25.2	-8	-9.8 (5-7)
HELIX 7	25.6	0.5	8.5	-21	6.22 (6-1)
AVERAGE	87.5	1.1	11.5	26	

The difference of these two crystal structures is easily seen in the shape and distribution of the hydrophobic character on each helix. The major structural difference is in helix 3 that in more inside the protein barrel on rhodopsin, but part of the outside barrel on bacteriorhodopsin (Figure 15).

5.0 DISCUSSION

With the growing interest in GPCRs, more structures of these proteins are being created from a number of different methods. These structures need a systematic approach to analyze the differences and characteristics of each to determine the usefulness of each. Seven key characteristics for describing the overall characteristics of these structures have been detailed in this paper: Helical bend, Helical tilt, HPM angle, Phobic face, and three characteristics to describing helical position.

These characteristics were then calculated for Bovine Rhodopsin, 8 Bacteriorhodopsin structures, and one theoretical model of D2 made from a Bacteriorhodpsin template. These key properties allowed the analysis of important details in the stability of the Rhodopsin structure with and without binding to cis-retinal. The dual characteristic of helix 3 for rhodopsin helps to understand the placement of this helix within the protein barrel having its hydrophobic character shift by 90 degrees to utilize the available interactions with the bilipid membrane.

The real benefit of this method for describing membrane proteins can be seen in the comparison of two proteins. From the 8 Bacteriorhodopsin structures, the one structure made from solution NMR data was immediately shown to be significantly different in the rotation and placement of sidechains on helices 4, 5, and 6. This might be due to the binding of retinal that was not present on the structure created from solution NMR data. The differences between Rhodopsin and Bacteriorhodopsin were shown to be significant even though both bind to retinal with a Lysine on TM 7. The most advantageous analysis came from comparing a theoretical structure to it's original template. The structure 1I15 was shown to be similar in structure to bacteriorhodopsin with differences only in the binding site residues for D2.

MembComp is a tool that allows the researcher to understand the important characteristics of the structure that they are working with. The properties developed in this method allow for the study of common characteristic trends that could appear in membrane proteins of similar families or similar function. This understanding of these trends will lead to the development of better theoretical models.

6.0 ACKNOWLEDGEMENTS

Special thanks to Nagarajan Vaidehi for asking if there was a better way to compare structures than using C-alpha RMS, and Deepshika Datta for the simulations done on crystal rhodopsin.

7.0 REFERENCES

1) Donnelly, D. (1993). Modeling alpha-helical transmembrane domains. *Biochem. Soc.* 21, 36–39.

2) Trabanino, R.J., Hall, S.E., Vaidehi N., Floriano W.B., and Goddard III W.A. (2004). First Principles Predictions of the Structure and Function of G-Protein Coupled Receptors: Validation for Bovine Rhodopsin. *BioPhys. J.* 2004 86, 1904-1921

3) Vaidehi, N.**,** Floriano, W. B., Trabanino, R., Hall, S. E., Freddolino, P., Choi, E. J., Zamanakos, G., and Goddard II, W. A. (2002). Prediction of structure and function of G protein-coupled receptors. *Proc. Nat. Acad. Sci*. 99(20), 12622-12627

4) Freddolino, P. L., Kalani, M. S. Y., Vaidehi, N., Floriano, W. B., Hall, S. E., Trabanino, R. J., Kam, W. T. and Goddard III, W. A. (2004). Predicted 3D structure for the human beta2 adrenergic receptor and its binding site for agonists and antagonists. *Proc. Natl. Acad. Sci.* 101, 2736-2741.

5) Kalani, M. Y. S., Vaidehi, N., Hall, S. E., Trabanino, R. J., Freddolino, P. L., Kalani, M. A., Floriano, W. B., Kam, V. W., and Goddard III, W. A. (2004). The predicted 3D structure of the human D2 dopamine receptor and the binding site and binding affinities for agonists and antagonists. *Proc. Natl. Acad. Sci.* 101, 3815-3820

6) Floriano W.B., Vaidehi, N., Singer M.S., Shepherd G.M., Goddard III, W.A. (2000). Molecular Mechanisms underlying differential odor responses of a mouse olfactory receptor. *P. Natl. Acad. Sci. USA* 97, 10712-10716.

7) Floriano, W. B., Vaidehi, N., and Goddard III, W. A. (2004). Making sense of olfaction through molecular structure and function prediction of olfactory receptors. *Chem. Senses* 29, 269-290.

8) Hall, Spencer E., Floriano, Wely B., Vaidehi, Nagarajan, and Goddard III, William A. (2004). Predicted 3-D Structures for Mouse I7 and Rat I7 Olfactory Receptors and Comparison of Predicted Odor Recognition Profiles with Experiment. *Chemical Senses* 29, 595–616.

9) Altschul, S. F., Gish, W., Miller, W., Myers, W. E., and Lipman, D. J. (1990). Basic local alignment search tool. *J. Mol. Biol.* 215, 403–410.

10) Altschul, S. F., Madden, T. L., Schaffer, A. A., Zhang, J., Zhang, Z., Miller, W., and Lipman, D. J. (1997). Gapped BLAST and PSI-BLAST: a new generation of protein database search programs. *Nucleic Acids Res.* 25, 3389–3402.

11) Thompson, J. D., Higgins, D. G., and Gibson, T. J. (1994). Clustal-W—improving the sensitivity of progressive multiple sequence alignment through sequence weighting, position-specific gap penalties and weight matrix choice. *Nucleic Acids Res*. 22, 4673–4680.

12) Eisenberg D., Weiss R.M., Terwilliger, T.C., (1984). The Hydrophobic Moment Detects Periodicity In Protein Hydrophobicity. *Proc. Natl. Acad. Sci. USA*, 8, 140-144.

13) Filizola, M., Perez, J. J., and Carteni-Farina, M. (1998). BUNDLE: A program for building the transmembrane domains of G-protein-coupled receptors. *Journal of Computer-Aided Molecular Design*. 12, 111-118.

14) Filizola, M., Carteni-Farina, M., and Perez, J. J. (1999). Modeling the #D Structure of Rhodopsin Using a De Novo Approach to Build G-protein-Coupled Receptors. *J. Phys. Chem. B*. 103, 2520-2527

15) Hall, S. E. (2005). PhD Thesis, California Institute of Technology

16) Datta, D. *Personal Communication.* Materials and Process and Simulation Center, California Institute of Technology

17) Lindahl, E., Hess, B., and van der Spoel, D. (2001). GROMACS 3.0: a package for molecular simulation and trajectory analysis, *J. Mol. Model.* 7, 306–317.

8.0 FIGURES

Figure 1. Displayed is the parallel plane that intersects the main structural elements of a GPCR. Notice that this plane can be positioned anywhere along the vertical axis (the axis that runs along the protein from the intracellular region to the extracellular region) of the protein.

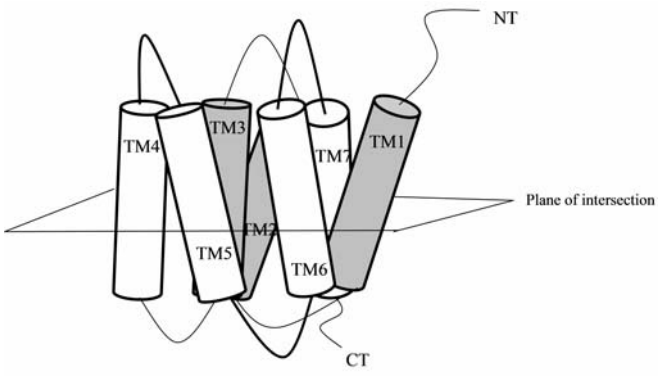

Figure 2. Plots of the MembStruk structure I7-Rat (8) with the C-alpha atoms projected onto the common planes of helices 3 and 7 and aligned to the circle of radius 1. The largest gap near the 1 on the X-axis corresponds to the Phobic Face angle for helix 3 and helix 7.

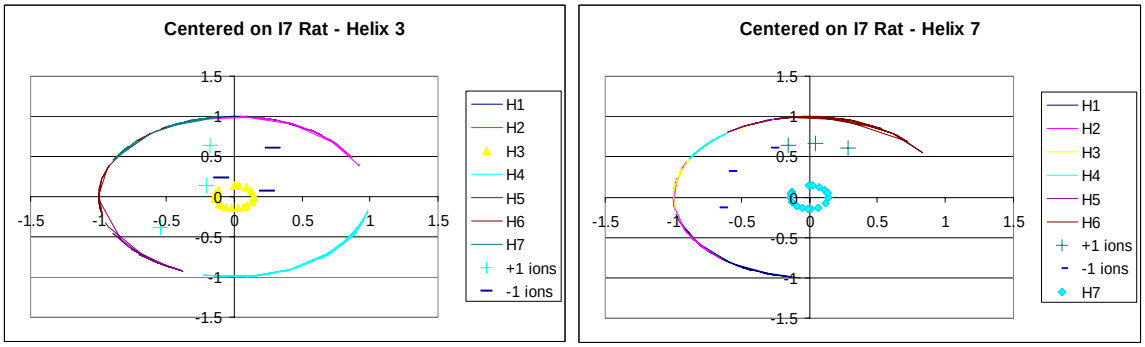

Figure 3. Plot of the summation of the windows 16 to 24 for bovine rhodopsin. The TM regions from the crystal structure are outlined by vertical lines, and the final peaks numbers are listed. These peaks aligned to a plane with an RMS of 0.5354 on the 1HZX crystal structure.

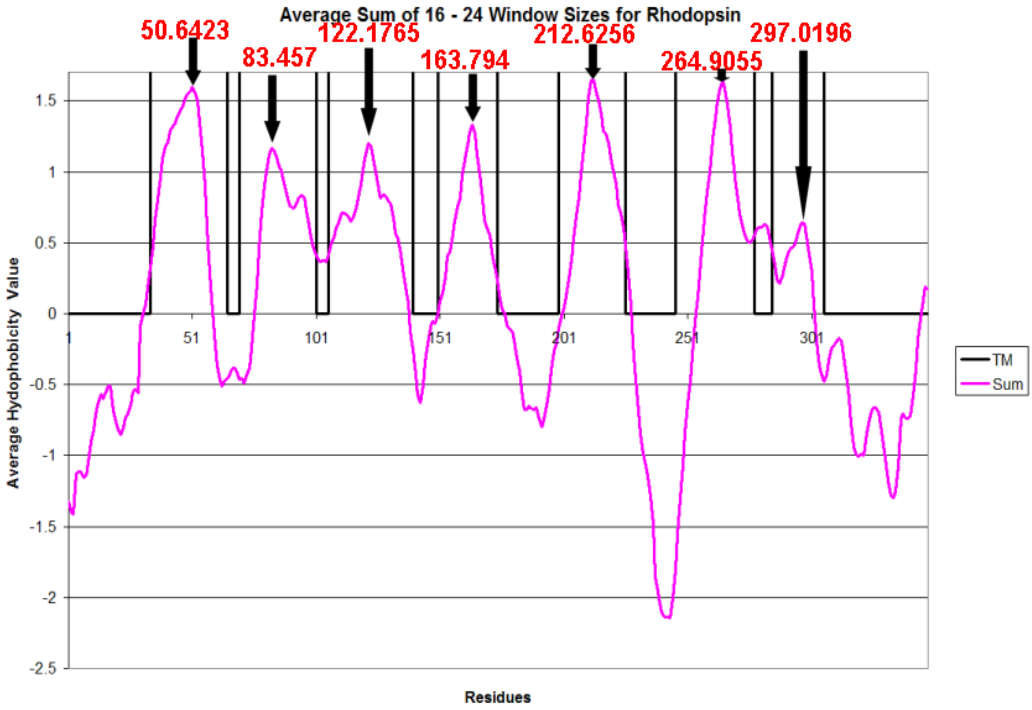

Figure 4. This is a plot of the summation of the window sizes 6 to 30 for Bacterhodopsin to determine the TM regions. Shown are the predicted TM regions and the helical regions given from the crystal structures.

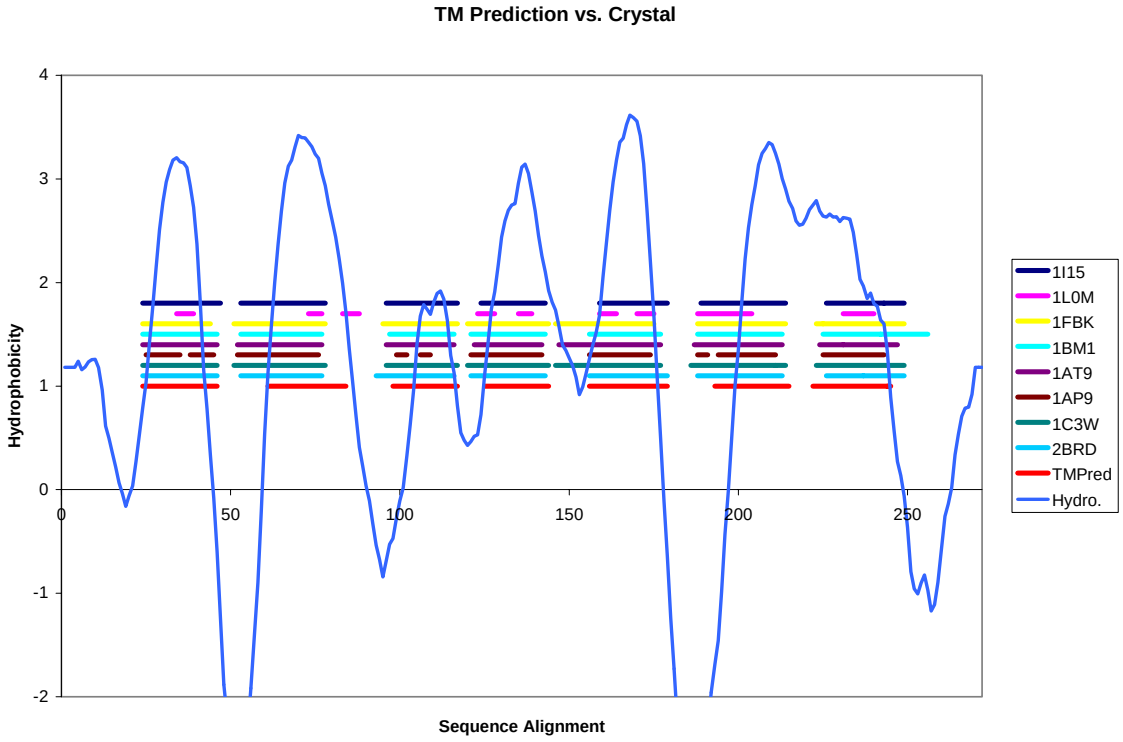

Figure 5. The window sizes for bacteriorhodopsin were each individually tested to find the alignment of the centers for each window size. For each window the largest peak and the next largest peak were found in the table below. Choosing from these two peaks, the peak closest to the center found by Get_Centers (1) gave the best fit to a plane of intersection. The final window sizes chosen for summation were: Helix 1 (14-24), Helix 2 (12-16), Helix 3 (22-28), Helix 4 (12-16), Helix 5 (12-16), Helix 6 (20-26), and Helix 7 (18-22). These window ranges were chosen based on consistency of the helical peaks found in those window sizes.

Bacteriorhodopsin HPM Centers											
	12	14	16	18	20	22	24	26	28	30	Ave of t
Helix 1	9/15	10/14	11/18	12	11/13	14/10	14/9	13/8	7/12	6/11	11.42
Helix 2	11/21	14/22	18/13	20/16	17/15	18/16	17/20	19/21	21/11	20/22	17.60
Helix 3	17/21	17/12	18/10	16/19	17/15	13/21	13/6	14/12	13/11	9/12	14.30
Helix 4	10/18	14/11	15/12	13/8	13/20	13/15	18/16	17/20	18/16	19/8	14.70
Helix 5	17/15	13/9	12/15	11/14	13/17	13/9	9/11	7/10	7/9	8/6	11.25
Helix 6	20/12	19/16	20/14	21/18	22/18	17/20	18/16	22/19	23/20	21/17	18.65
Helix 7	5/14	15/13	14/9	13/8	11/7	10/6	8/16	9/16	8/13	7/13	10.75
Plane Fit	2.7	3.98	4.82	4.44	3.7	2.2	3	3.24	3.53	1.89	2.38
All sm pks	3.73	3.67	3.69	2.62	5.21	4.53	2.2	3.79	2.49	4.99	
Closest to	3.25	1.47	2.00	2.95	2.08	1.32	2.29	2.54	2.56	3.93	

* Highest peak / 2nd highest peak

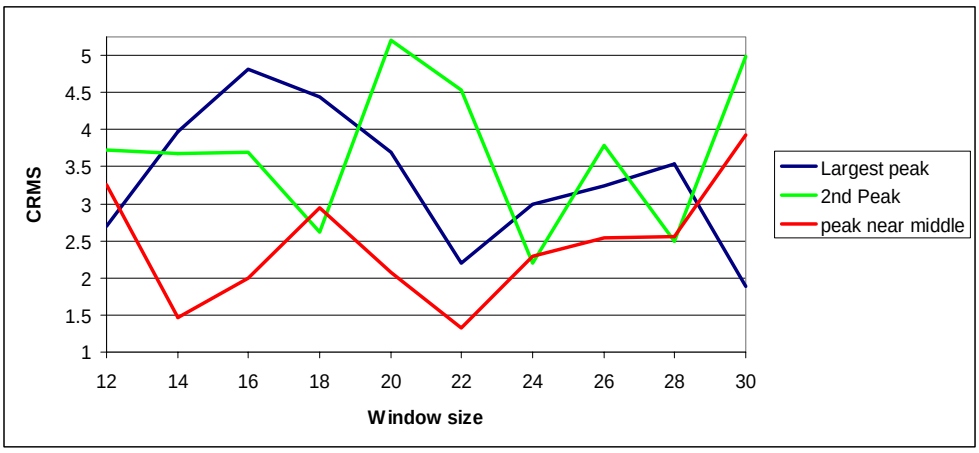

Figure 6. Graph of the key properties of bovine rhodopsin (1HZX) using the summed set of hydrophobic centers seen in figure 3. Shown are the key properties as plotted on the plane of intersection. The lines represent the projected helical tops (marked with a "t"), centers, and bottoms to give an idea of the helical tilt (if the tilt was 0, then there would be no line) and helical bend. The circles around the helical centers represent how far away the center is from the plane of intersection, with the thicker circles being on the extracellular side.

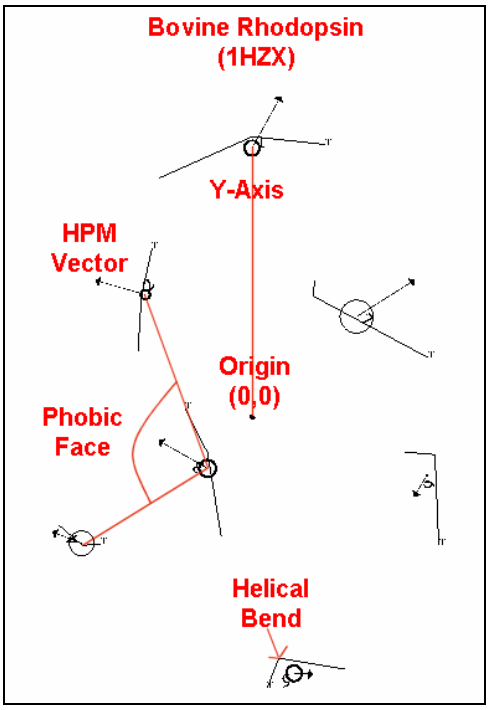

Figure 7. Shown here is the HPM vectors from the centered plane on helix3 for bovine rhodopsin (1HZX). The black represents the key properties found on the centered plane for the top (extracellular) 15 residues above the HPM center of helix 3. The green represents the key properties found on the centered plane for the bottom (intracellular) 15 residues below the HPM center of helix 3.

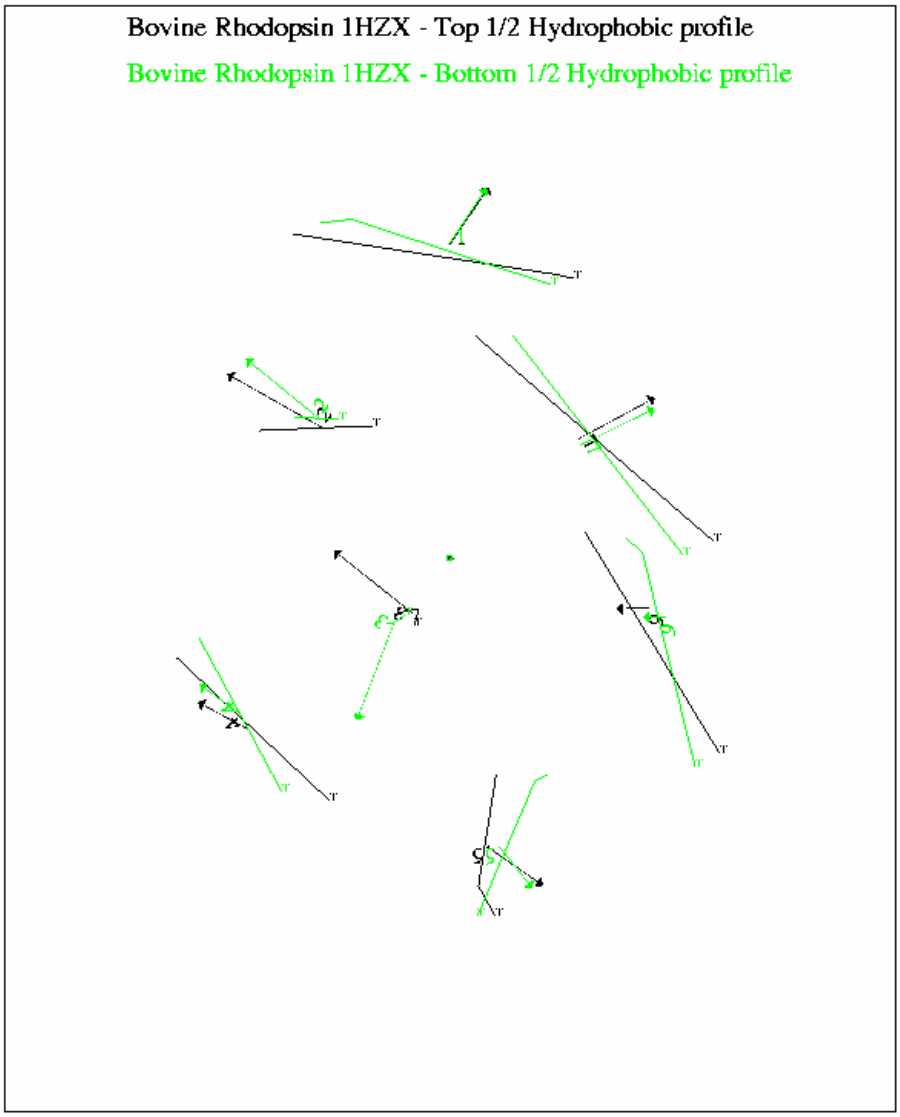

Figure 8. The Binding site analysis around the summed hydrophobic moments for 1hzx Bovine Rhodopsin with bound cis-retinal. Shown are only the HPM vectors for the five nearest residues to each helix's hydrophobic center. Plotted are the key residues found in the binding site of cis-retinal (1). The residue dot represents the geometric center of the end atoms of the residue projected onto the hydrophobic center plane with the number of the TM region and the aminoacid letter code for each residue. The black circles represent the centers of the helices, and **black** letters are aromatic residues. Blue represents the hydrophilic residues and green represents all other residues. Purple is the heavy atoms for cis-retinal.

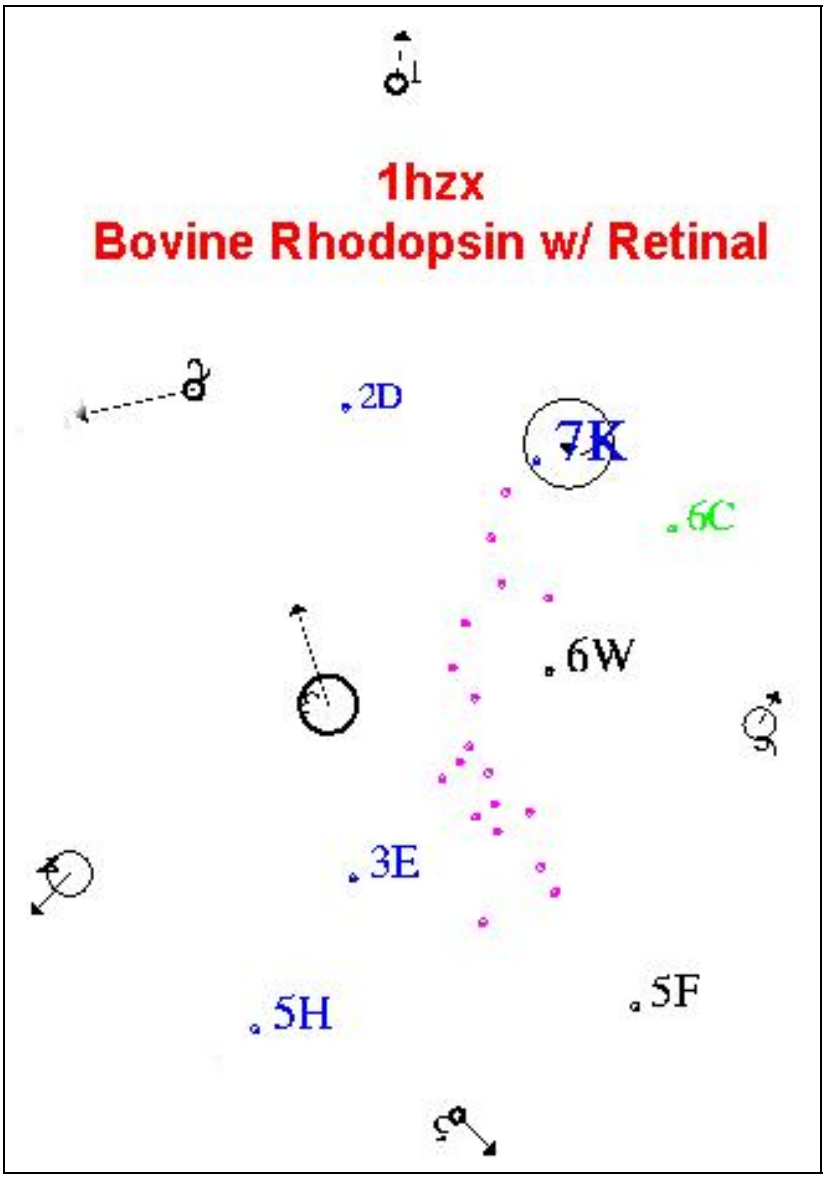

Figure 9. Plotted are the calculated HPM angles on the common helical plane for the four simulations carried out on 1F88 crystal bovine rhodopsin. The starting HPM angles for 1F88 are: H1 -5.6, H2 5.5, H3 -55.7, H4 -57.5, H5 82.1, H6 -55.4, and H7 -33.6 from MembComp 1.56.

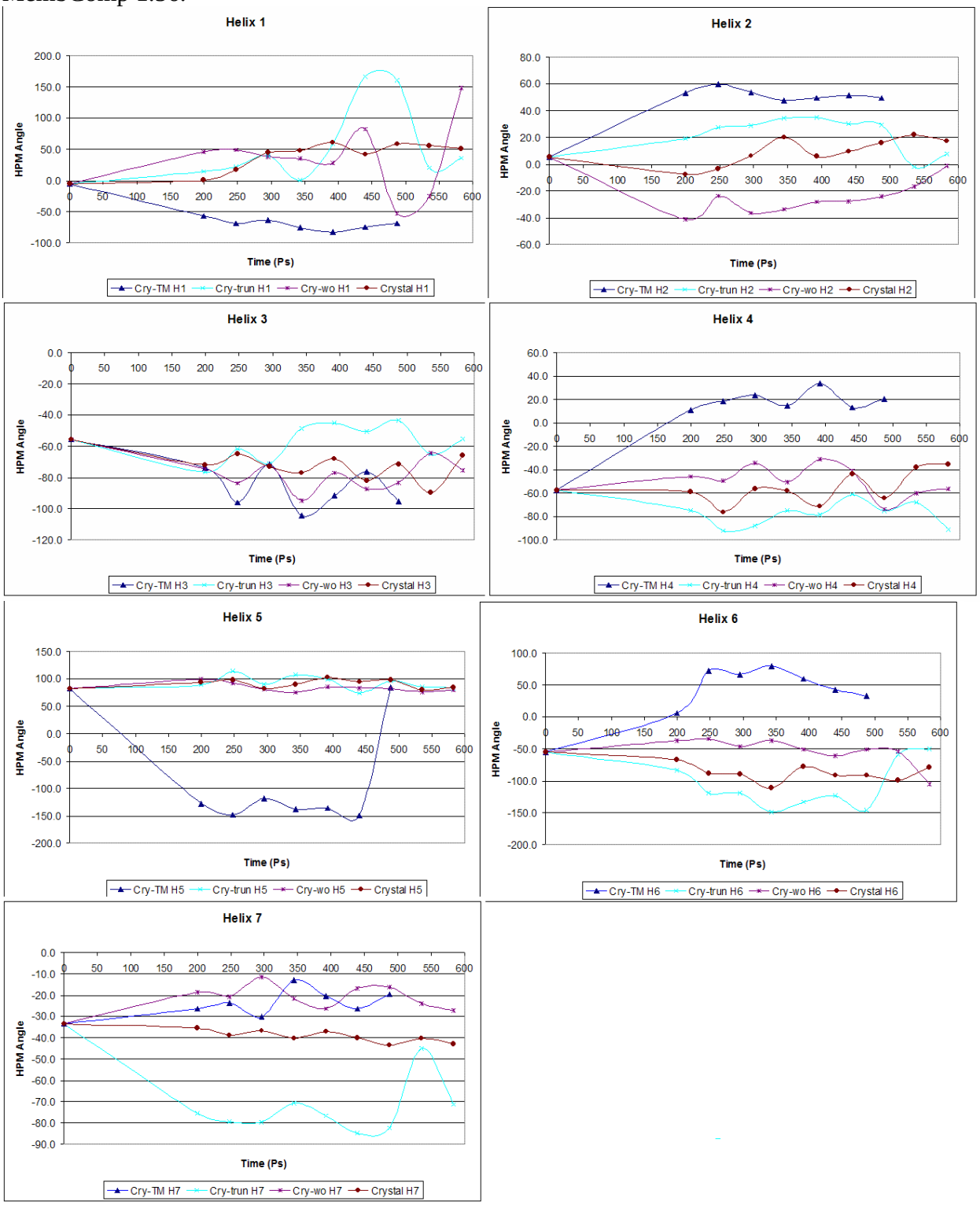

Figure 10. Plotted are the calculated helical tilts on the plane of intersection for the four simulations carried out on 1F88 crystal bovine rhodopsin. The starting helical tilts for 1F88 are: H1 22.5, H2 13.6, H3 22.4, H4 2.2, H5 18.6, H6 25.8, and H7 30.2 from MembComp 1.56.

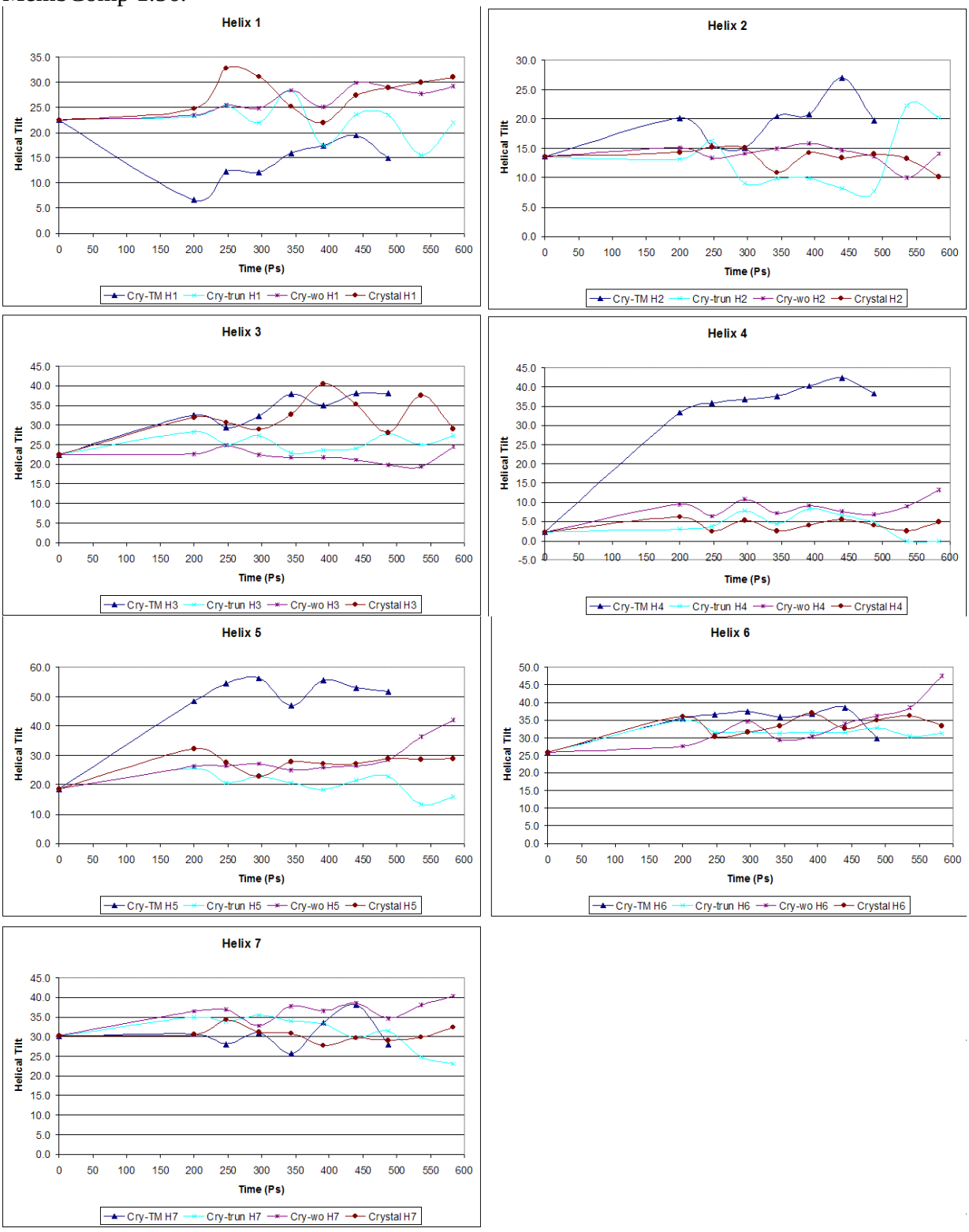

Figure 11. Plotted are the calculated helical bends on the plane of intersection for the four simulations carried out on 1F88 crystal bovine rhodopsin. The starting helical bends for 1F88 are: H1 13.4, H2 4.3, H3 11.5, H4 11.4, H5 24.0, H6 27.4, and H7 33.7 from MembComp 1.56.

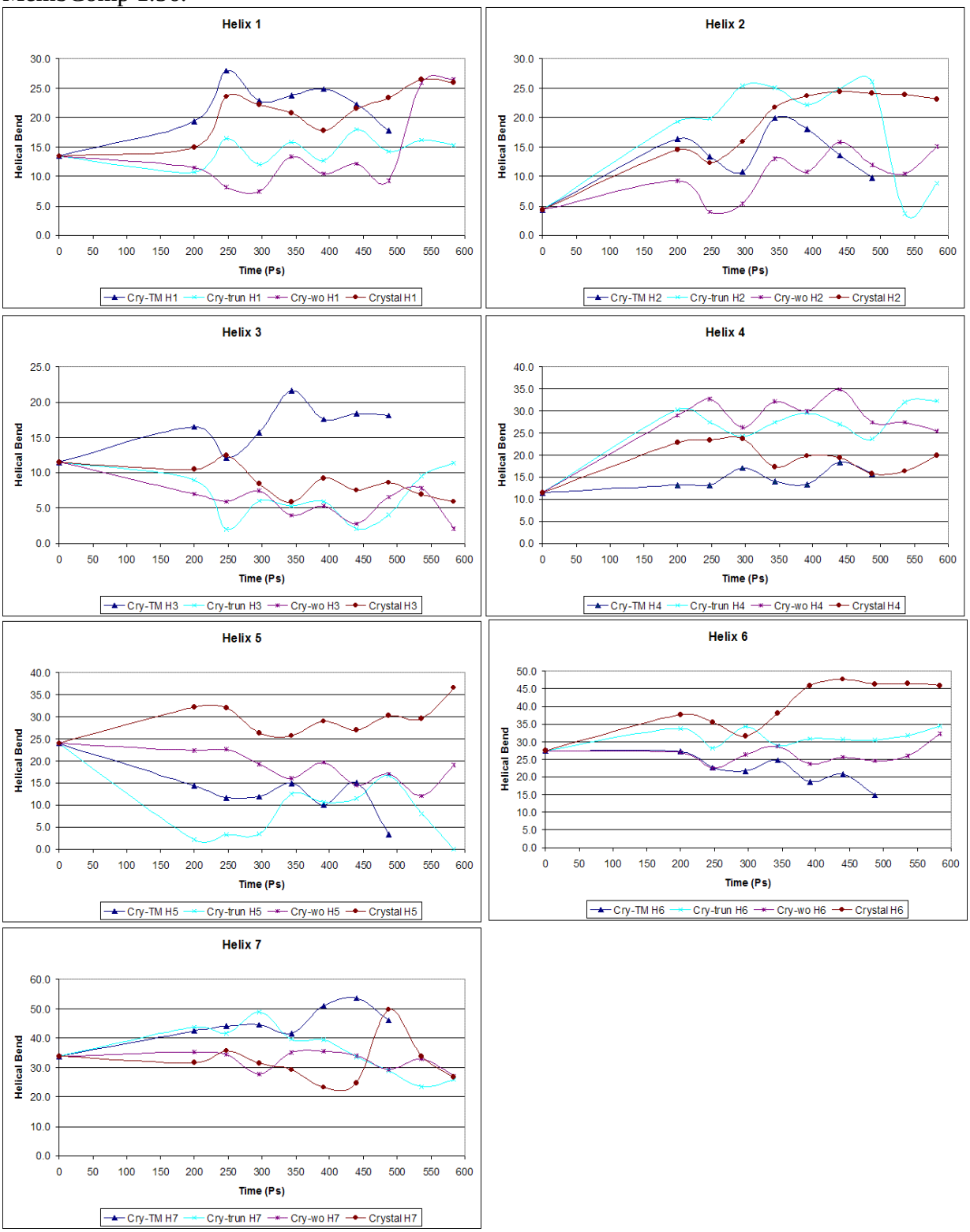

Figure 12. Using the HPM centers for Bacteriorhodopsin, the key properties for the nine structures were calculated and plotted together. 1I15 can be seen to be different in helices 4, 5, and 6.

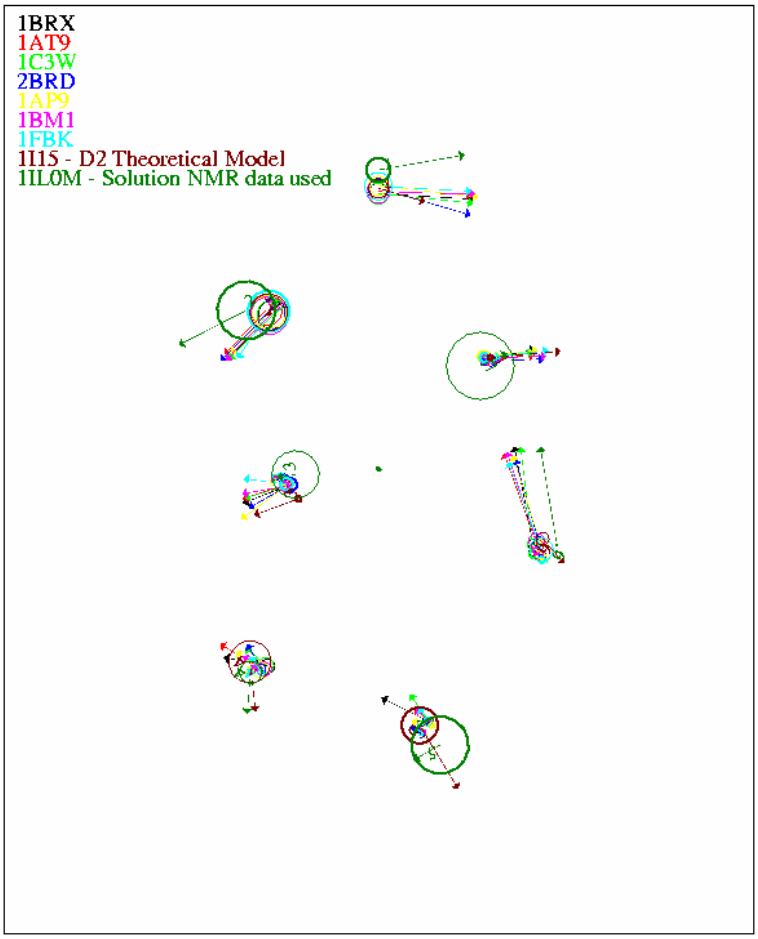

Figure 13. Shown are close-ups of helices 4, 5, and 6 of figure 8.

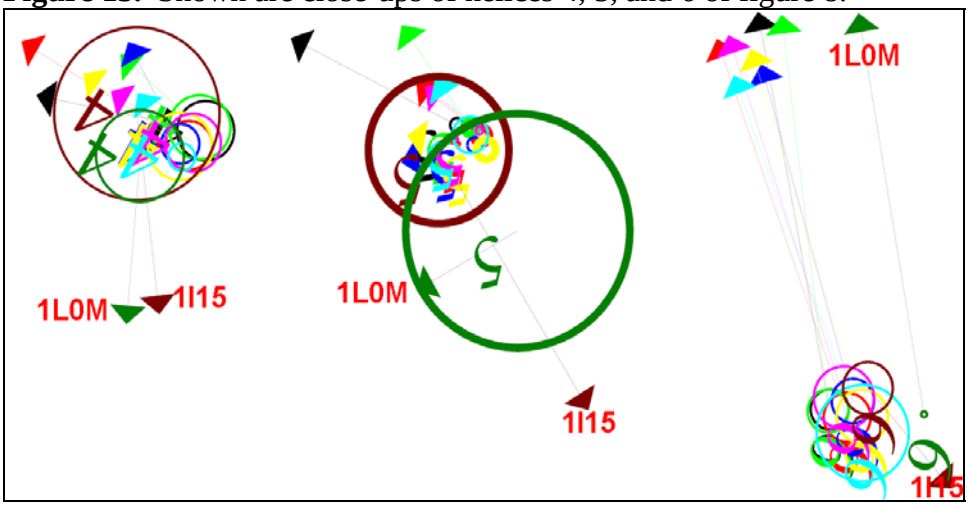

Figure 14. The Binding site analysis around the summed hydrophobic moments for 1C3W Bacteriorhodopsin with retinal. Plotted are the close residues found in the binding site of retinal. The residue dot represents the geometric center of the end atoms of the residue projected onto the hydrophobic center plane with the number of the TM region and the aminoacid letter code for each residue. The black circles represent the centers of the helices, and **black** letters are aromatic residues. Blue represents the hydrophilic residues and green represents all other residues. Purple is the heavy atoms for retinal.

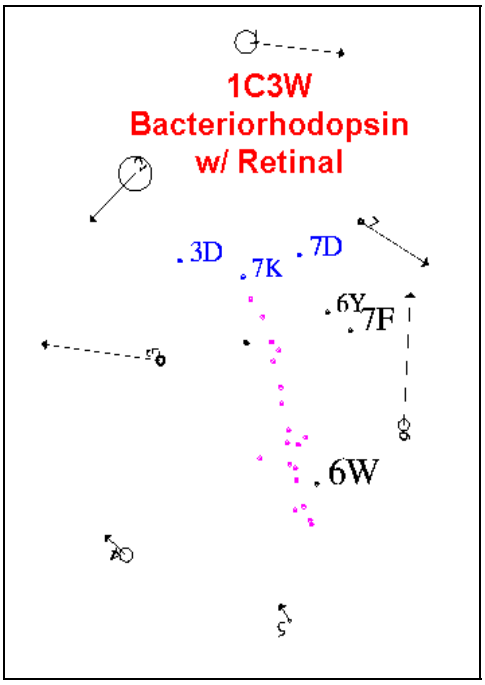

Figure 15. Plotted comparison of Rhodopsin and Bacteriorhodopsin.